

Preceding page blank

173-1014

12: A Dynamic Model of the Human Postural Control System*

J. C. HILL

Oakland University

A digital simulation of the pitch axis dynamics of the stick man of figures 1 and 2 is described. Difficulties encountered in linearizing the equations of motion are discussed; the conclusion reached is that a completely linear simulation is of such restricted validity that only a nonlinear simulation is of any practical use.

Typical simulation results obtained from the full nonlinear model are presented in this paper.

INTRODUCTION

In reference 1 the equations of motion of the seven-element linked figure of figures 1 and 2 were derived. The links represent the trunk, thigh, shank, foot, upper arm, forearm, and head as seen in a side view of the human body. Each link is considered to have mass and rotational inertia. Thus for the trunk, we have a link of total length ℓ_{TR} , moment of inertia J_{TR} , and mass M_{TR} , located at the trunk center of mass, which is a distance ℓ_{TRM} , above the hip. Similar nomenclature is used to define the properties of the other links. The trunk orientation is described in terms of the x and y coordinates of the trunk c.g. and the rotation θ of the trunk center line clockwise from the vertical. All other limb orientations are described by angles as shown in figure 1.

In figure 2, a preliminary model of the forces and torques acting on the seven-element stick man of figure 1 is shown. The muscle systems are assumed to produce torques T_α about the ankle, T_β about the knee, etc. It is assumed that both the heel and toe can be in contact with the ground, where the x and y components of the ground reaction forces acting on the model are F_{H_x} and F_{H_y} at the heel, and F_{T_x} and F_{T_y} at the toe.

*This research was supported by NASA under contract NGR 23-054-033.

Gravitational forces acting at the centers of mass of each link are not shown.

The preceding constitutes the definition of a possible set of generalized coordinates in the sense of Lagrange.

LAGRANGE'S EQUATIONS

To develop the equations of motion of the postural control system model shown in figures 1 and 2, use was made of Lagrange's equations in the form of equation (1),

$$\frac{d}{dt} \left(\frac{\partial T}{\partial \dot{q}_i} \right) - \frac{\partial T}{\partial q_i} + \frac{\partial V}{\partial q_i} = Q_i \quad i = 1, 2, \dots, n \quad (1)$$

where q_i denotes the i^{th} generalized coordinate (taken here in the order $(x, y, \theta, \gamma, \beta, \alpha, \delta, \epsilon, \zeta)$), \dot{q}_i is the time derivative of the i^{th} generalized coordinate, V is the total potential energy of the system, T is the total kinetic energy of the system, and Q_i is the i^{th} generalized force arising from the muscle torques and the ground reaction forces. Gravitational forces are included through the potential energy V . Hence expressions for T and V in terms of the generalized coordinates and their derivatives must be derived, the indicated differentiations with respect to q_i , \dot{q}_i , and t must be carried out for $i = 1, \dots, n$, the generalized forces must be evaluated, and the results collected according to equation (1).

The resulting equations are far too lengthy for

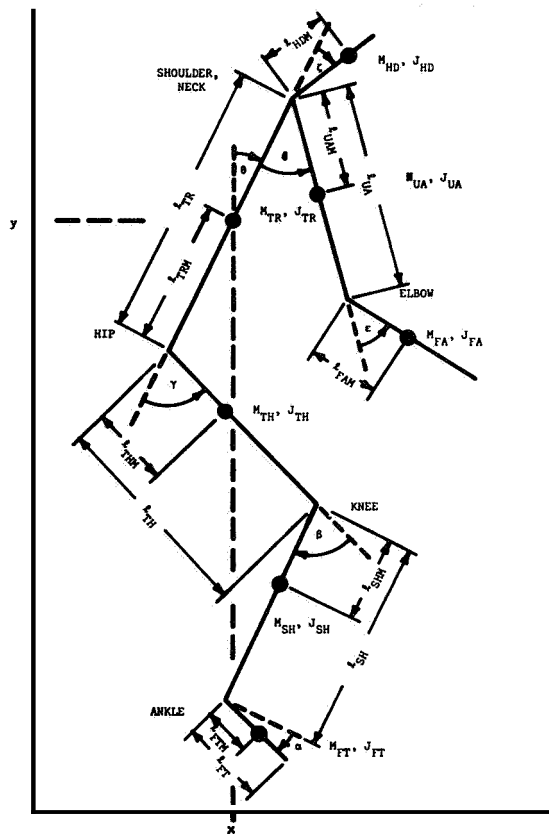


FIGURE 1.—Seven-element linked model of the human postural control system.

inclusion here. They are contained in their entirety in reference 1.

LINERIZATION

For a variety of reasons, it would appear desirable to have a linear model valid for small deflections. First, standard techniques from linear control theory are available to assist in designing control laws for the system. Second, a linear model would be much easier to simulate on an analog computer, and the speed possible from an all-analog simulation is much to be desired in future work. Third, if a linear model is acceptable, considerable algebraic simplification in the preceding equations may be achieved by keeping only terms of degree one or less.

The results thus obtained may best be represented in the form of the vector-matrix differential equation

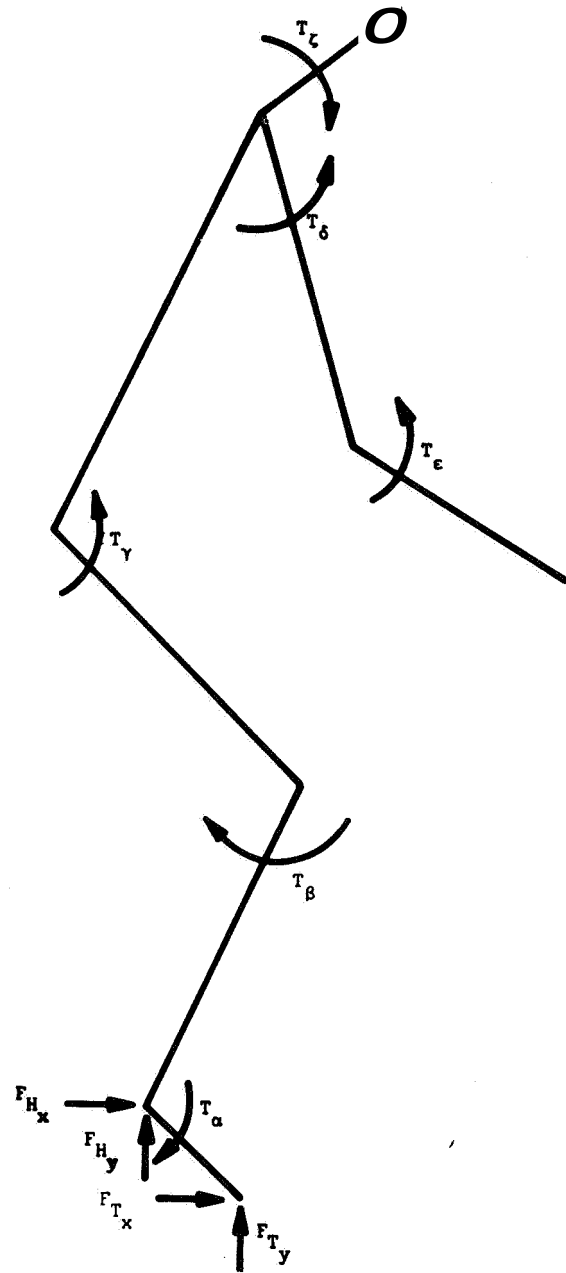


FIGURE 2.—Forces and torques acting on the postural control system.

$$A\ddot{x} = C\dot{x} + y \tag{2}$$

where A is a square matrix of order 9×9 , C is a square matrix of order 9×9 , and x and \dot{x} are 9-vectors whose components are defined in equation (3),

$$x = \begin{Bmatrix} x \\ y \\ \theta \\ \gamma \\ \beta \\ \alpha \\ \delta \\ \epsilon \\ \zeta \end{Bmatrix}, \quad \ddot{x} = \begin{Bmatrix} \ddot{x} \\ \ddot{y} \\ \ddot{\theta} \\ \ddot{\gamma} \\ \ddot{\beta} \\ \ddot{\alpha} \\ \ddot{\delta} \\ \ddot{\epsilon} \\ \ddot{\zeta} \end{Bmatrix} \quad (3)$$

and y is a 9-vector of constants.

For the parameter values given in table 1, which are rough estimates of the lengths, masses, and inertias appropriate to a 160 lb man, A , C , and v may be estimated as shown below.

From equation (4), since A is not diagonal, equation (2) is badly cross coupled in the accelerations; an analog computer programmer would say that equation (2) has an algebraic loop problem. Although algebraic loops on an analog computer usually are troublesome only if they

TABLE 1.—Numerical Parameter Estimates for a 160 lb Man

$M_{TR} = 2.1$ slugs.....	$\ell_{TR} = 2.0$ ft
$M_{TH} = 1.3$ slugs.....	$\ell_{TH} = 1.3$ ft
$M_{SH} = 0.6$ slug.....	$\ell_{SH} = 1.5$ ft
$M_{FT} = 0.1$ slug.....	$\ell_{FT} = 0.6$ ft
$M_{UA} = 0.4$ slug.....	$\ell_{UA} = 1.0$ ft
$M_{FA} = 0.2$ slug.....	$\ell_{TRM} = 1.2$ ft
$M_{HD} = 0.3$ slug.....	$\ell_{THM} = 0.5$ ft
$J_{TR} = 0.5$ slug-ft ²	$\ell_{SHM} = 0.6$ ft
$J_{TH} = 0.25$ slug-ft ²	$\ell_{FTM} = 0.2$ ft
$J_{SH} = 0.1$ slug-ft ²	$\ell_{UAM} = 0.4$ ft
$J_{FT} = 0.01$ slug-ft ²	$\ell_{FAM} = 0.4$ ft
$J_{UA} = 0.05$ slug-ft ²	$\ell_{HDM} = 0.8$ ft
$J_{FA} = 0.02$ slug-ft ²	
$J_{HD} = 0.03$ slug-ft ²	$g = 32.18$ ft/sec ²

lead to instability in the solutions, numerical integration of equation (2) requires that the coupling be removed (actually, it is only necessary that the matrix multiplying \ddot{x} be lower left-

$$A = \begin{bmatrix} 5.000 & 0.000 & -3.949 & 2.069 & -0.509 & 0.000 & 0.439 & 0.079 & 0.239 \\ 0.000 & 5.000 & -0.019 & 0.019 & -0.019 & -0.019 & 0.000 & 0.000 & 0.000 \\ -3.949 & -0.019 & 12.990 & -6.122 & 1.829 & 0.014 & -0.173 & -0.067 & 0.413 \\ 2.069 & 0.019 & -6.122 & 3.638 & -1.217 & -0.014 & 0.000 & 0.000 & 0.000 \\ -0.509 & -0.019 & 1.829 & -1.217 & 0.554 & 0.014 & 0.000 & 0.000 & 0.000 \\ 0.000 & -0.019 & 0.014 & -0.014 & 0.014 & 0.014 & 0.000 & 0.000 & 0.000 \\ 0.439 & 0.000 & -0.173 & 0.000 & 0.000 & 0.000 & 0.525 & 0.131 & 0.000 \\ 0.079 & 0.000 & -0.067 & 0.000 & 0.000 & 0.000 & 0.131 & 0.052 & 0.000 \\ 0.239 & 0.000 & 0.413 & 0.000 & 0.000 & 0.000 & 0.000 & 0.000 & 1.221 \end{bmatrix} \quad (4)$$

$$C = \begin{bmatrix} 0.000 & 0.000 & 0.000 & 0.000 & 0.000 & 0.000 & 0.000 & 0.000 & 0.000 \\ 0.000 & 0.000 & 0.000 & 0.000 & 0.000 & 0.000 & 0.000 & 0.000 & 0.000 \\ 0.000 & 0.000 & -127.110 & 0.000 & 0.000 & 14.159 & 2.574 & 7.723 & 0.000 \\ 0.000 & 0.000 & 66.612 & 0.000 & 0.000 & 0.000 & 0.000 & 0.000 & 0.000 \\ 0.000 & 0.000 & -16.411 & 0.000 & 0.000 & 0.000 & 0.000 & 0.000 & 0.000 \\ 0.000 & 0.000 & 0.000 & 0.000 & 0.000 & 0.000 & 0.000 & 0.000 & 0.000 \\ 0.000 & 0.000 & 14.159 & 0.000 & 0.000 & -14.159 & -2.574 & 0.000 & 0.000 \\ 0.000 & 0.000 & 2.574 & 0.000 & 0.000 & -2.574 & -2.574 & 0.000 & 0.000 \\ 0.000 & 0.000 & 7.723 & 0.000 & 0.000 & 0.000 & 0.000 & 7.723 & 0.000 \end{bmatrix} \quad (5)$$

$$v = \begin{Bmatrix} 0.000 \\ -160.899 \\ 0.643 \\ -0.643 \\ 0.643 \\ 0.643 \\ 0.000 \\ 0.000 \\ 0.000 \end{Bmatrix} \quad (6)$$

half triangular, for then each acceleration may be solved for in sequential fashion). Complete decoupling may be achieved by premultiplication of equation (2) by A^{-1} , yielding equation (7):

$$\begin{aligned} A^{-1}(A\ddot{x}) &= A^{-1}(C\dot{x}) + A^{-1}y \\ I\ddot{x} &= (A^{-1}C)\dot{x} + A^{-1}y \\ \ddot{x} &+ (A^{-1}C)\dot{x} + A^{-1}y \end{aligned} \quad (7)$$

The matrices A^{-1} , $A^{-1}C$, and the vector $A^{-1}y$ are shown below.

It is of interest to note that although A , C , and A^{-1} are symmetric, $A^{-1}C$ is not. Symmetry (or lack of it) has proved useful in ferreting out errors in A and C .

MODEL VALIDATION: THE FREE FALL TESTS

In view of the large amount of hand derivation and computer programming involved in the development of equations (7 through 10), it is clearly desirable to test the model to see if it is at all reasonable. As no provision has been made for the addition of external forces and/or torques via the generalized forces of equation (1) at this stage in the analysis, one is limited to free fall conditions, several of which may be defined:

- (1) Free fall with zero initial conditions on all angles
- (2) Free fall with a small initial condition, say 0.1 radian, on only one angle at a time

$$A^{-1} = \begin{bmatrix} 0.366 & 0.000 & 0.130 & -0.076 & -0.263 & 0.056 & -0.454 & 0.759 & -0.640 \\ 0.000 & 0.201 & 0.000 & 0.000 & 0.000 & 0.287 & -0.000 & 0.000 & -0.000 \\ 0.130 & -0.000 & 0.713 & 1.431 & 0.912 & -0.195 & -0.157 & 1.130 & -1.472 \\ -0.076 & -0.000 & 1.431 & 4.262 & 4.610 & -1.779 & 0.105 & 1.721 & -2.586 \\ -0.263 & 0.000 & 0.912 & 4.610 & 8.796 & -5.098 & 0.334 & 0.751 & -1.417 \\ 0.056 & 0.287 & -0.195 & -1.779 & -5.098 & 75.354 & -0.071 & -0.160 & 0.303 \\ -0.454 & -0.000 & -0.157 & 0.105 & 0.334 & -0.071 & 5.800 & -14.230 & 0.783 \\ 0.759 & -0.000 & 1.130 & 1.721 & 0.751 & -0.160 & -14.230 & 55.663 & -2.930 \\ -0.640 & -0.000 & -1.472 & -2.586 & -1.417 & 0.303 & 0.783 & -2.930 & 7.942 \end{bmatrix} \quad (8)$$

$$A^{-1}C = \begin{bmatrix} 0.000 & 0.000 & -26.815 & 9.484 & 0.926 & 0.000 & 6.325 & -0.449 & -3.934 \\ 0.000 & 0.000 & 0.000 & -0.000 & -0.000 & 0.000 & 0.000 & -0.000 & -0.000 \\ 0.000 & 0.000 & -21.043 & -32.815 & -3.205 & 0.000 & 9.418 & -0.669 & -5.858 \\ 0.000 & 0.000 & 12.325 & -112.958 & -29.198 & 0.000 & 14.338 & -1.019 & -8.920 \\ 0.000 & 0.000 & 42.453 & -101.959 & -83.683 & 0.000 & 6.260 & -0.445 & -3.894 \\ 0.000 & 0.000 & -9.083 & 21.816 & 57.690 & 0.000 & -1.339 & 0.095 & 0.833 \\ 0.000 & 0.000 & 73.056 & -12.007 & -1.173 & 0.000 & -47.714 & 21.297 & 4.840 \\ 0.000 & 0.000 & -122.207 & -27.022 & -2.639 & 0.000 & 74.198 & -103.755 & -13.895 \\ 0.000 & 0.000 & 103.021 & 50.942 & 4.976 & 0.000 & -24.401 & 1.734 & 49.969 \end{bmatrix} \quad (9)$$

$$A^{-1}y = \begin{bmatrix} -0.000 \\ -32.179 \\ -0.000 \\ 0.000 \\ 0.000 \\ 0.000 \\ 0.000 \\ -0.000 \\ 0.000 \end{bmatrix} \quad (10)$$

(3) Free fall with a small initial condition, say 0.1 radian, on all angles.

Tests (1), (2), and (3) provide a sequence of increasingly severe tests that the simulation must pass.

In test (1), the model is initially "lined out," and would be expected to remain that way since there are no forces or torques other than gravitational forces acting on the system. Test (1) essentially verifies that the origin of the state space is indeed an equilibrium point.

Test (2) allows the system to be perturbed from its equilibrium point in one coordinate at a time. Test (2) is, in essence, a test of the stability of the equilibrium point under restricted conditions. Intuitively, one would expect the perturbed angle to remain at its initial value of 0.1 radian while all other angles remain at their initial value of zero.

Finally, test (3) allows a general perturbation of the system from its equilibrium point. Intuitively, one again expects no action—all angles should remain at their initial values as the model drops straight down in free fall.

Several comments about these tests are in order. First, it might be argued that the system is linear. Therefore either test (2) or test (3) is redundant—they both give the same information. Although this is true of the way the simulation *ought* to behave, it is not necessarily true of how the simulation *does* behave, the difference presumably being due to a mistake somewhere. Both tests (2) and (3) are therefore useful in debugging the simulation.

Secondly, with the initial conditions of, say, test (3) one would not necessarily expect the angles to remain *precisely* at their initial values. An exact simulation of the physical system would be expected to do so, but the model presently under discussion is inexact in at least three ways:

(1) The equations have been linearized, and are therefore valid for small deflections only.

(2) A numerical integration technique (Runge-Kutta or Euler) is used, which inherently produces only approximations to the exact solution.

(3) Even if (1) and (2) were not a factor, the finite word length of a digital computer introduces errors into the results.

Strange or unwelcome behavior of a properly coded simulation can usually be identified as

arising from one or another of these three causes by making use of the following properties of each type of error:

(1) Errors due to linearization only become smaller as the system variables remain closer to their equilibrium point. Hence these errors can be made as small as desired by the simple expedient of assuming smaller initial conditions. Behavior of the linear system should approach behavior of the nonlinear system as the initial conditions are made smaller and smaller.

(2) Functional truncation errors introduced by the integration technique used tend to zero as the integration step size approaches zero. Subject only to consideration of the amount of machine time required, these errors usually may be made as small as desired.

(3) Errors introduced by the finite word length of the computer used can usually be eliminated or at least estimated by running the simulation in extended or double precision. If the arithmetic precision can, practically speaking, be extended without limit, these truncation errors can, practically speaking, be reduced without limit. Again, the only real consideration often is the increased running time implied thereby.

In summary.—Provided that the initial conditions on the angles are small enough, provided that the integration step size is small enough, and provided that the word length used is long enough, it would be expected that the linear simulation angles would, at worst, drift *slowly* away from their initial values if indeed the exact solutions were constant. Fast changes in θ , γ , α , . . . would be interpreted as behavior common to the approximate linear model and the exact nonlinear system.

Application of the Free Fall Tests to the Linear Model

In figure 3, time histories of the joint angles are presented for the initial conditions of test (3). It is seen that by the time only 100 msec have passed, the angles have departed from their initial value of 0.1 radian by amounts up to 80 percent. During this time, the system has fallen 0.14 ft or only about 1.6 in.

In comparison, figure 4 presents the time his-

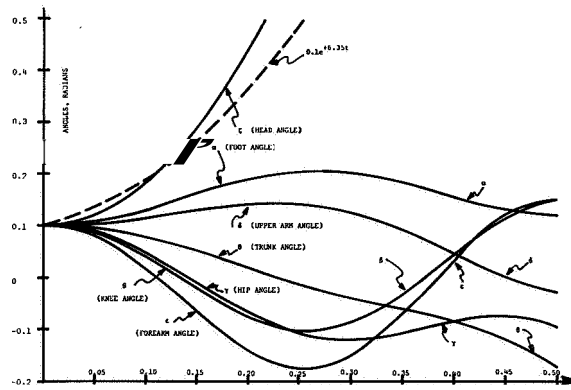


FIGURE 3.—Linear model, test (3): 0.1 radian initial conditions on each angle.

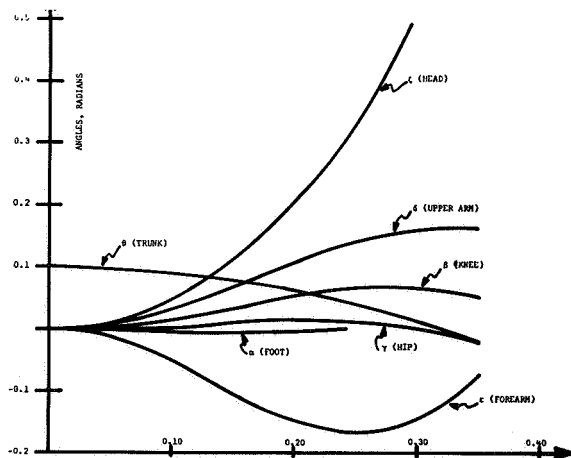


FIGURE 4.—Linear model, test (2): 0.2 radian initial condition on θ only.

tories of the angles for a typical test (2): an initial condition of 0.1 radian is placed on θ , and all other angles are set to zero initial conditions. The simulation is allowed to free fall, θ drifts away from 0.1 radian, and the other angles move relatively rapidly away from zero.

The system is a (constantly) forced linear system, and it is not immediately apparent whether the divergences seen in figures 3 and 4 are a result of instability of the model or are in response to the forcing function (gravity) or perhaps both. Accordingly, the pole locations of the linear system were calculated, and are given in table 2. The Linear Approximating System (LAS) has six poles at the origin, five pure imaginary pole pairs with natural frequencies ranging

TABLE 2.—Linear Approximating System Pole Locations in the Complex Plane

Real	Imaginary
0	0 (multiplicity=6)
0	$\pm j 12.32$
0	$\pm j 11.03$
0	$\pm j 6.71$
0	$\pm j 5.42$
0	$\pm j 3.35$
+6.35	0
-6.35	0

from $\sqrt{3.35}$ to $\sqrt{12.32}$, and two real poles—one stable at -6.35 , one unstable at 6.35 . It is clear that for large t the initial condition response will be dominated by the $e^{6.35t}$ term associated with the unstable pole. For comparison purposes, $0.1e^{+6.35t}$ is plotted on figure 3, and appears to be closely connected to the response of the head.

The fact that the behavior presented in figures 3 and 4 is substantially independent of the magnitude of the initial conditions, substantially independent of integration step size, and substantially independent of word length, together with the fact that during the 100 msec or so it takes the angles to depart significantly from their theoretical values the simulation has time to fall only 0.14 ft or 1.6 in. precludes interpretation of these changes as the slow drifts from the exact solution discussed in the preceding section. If the possible causes of error are only those previously discussed and if the observed behavior cannot be accounted for in terms of these causes, then it would appear that we are suffering from a different kind of not-so-sophisticated error—the mistake.

Accordingly, the results of figures 3 and 4 triggered an extensive and arduous period of differentiation-checking, algebra-checking, coefficient-checking, and program-checking including two completely different derivations and programs developed independently—all in an attempt to find the mistake and all to no avail. The results lead inexorably to the conclusion that the analysis leading to equations (3) and (4), and the pole locations given in table 2 are completely correct (useless, maybe—but correct). Either our intuition is wrong and the physical system really

behaves as shown in figures 3 and 4, or there is some other as yet unappreciated explanation of the discrepancy. The system clearly knows what it is doing.

Investigation of some simpler systems led to the conclusion that a completely linear simulation would be of such restricted validity as to be essentially useless. Consequently, the full nonlinear equations of motion were derived (ref. 1); the next section presents preliminary results obtained with this model.

SIMULATION RESULTS WITH THE FULL NONLINEAR MODEL

In this section simulation results of the following three physical situations will be presented. These simulations utilize the full nonlinear equations of motion.

(1) *Free fall with no muscle torques.*—The model is in free fall until it touches the ground, after which it collapses under the action of the ground reaction forces and gravity (fig. 5). Figures 6 and 7 are strip charts of free fall data.

(2) *Stand erect.*—Muscle torques proportional to a linear combination of joint angle and joint angular rate are applied so as to attempt drive all joint angles to zero, resulting in a stable upright position (fig. 8).

(3) *The leap.*—The control laws specifying muscle torques are modified to cause the hip and thigh to extend and the foot to deflect in such a way as to propel the model back into the air after impact in an imitation of a "graceful leap" (fig. 9).

Simulation Results: Free Fall With No Muscle Torques

Figure 5 is the result of releasing the model slightly above the ground in a slightly deflected attitude. The system configuration is drawn at 30 msec intervals. The sequence of events can easily be identified: the toe hits, the vertical ground reaction at the toe causes the foot to flex around the ankle, eventually the heel hits, initiating significant flexure of the hip and knee, etc. It should be remembered that the muscle system is not attempting to oppose the tendency of the model to collapse on the ground since all muscle torques (T_α , T_β , . . .) have been set to zero.

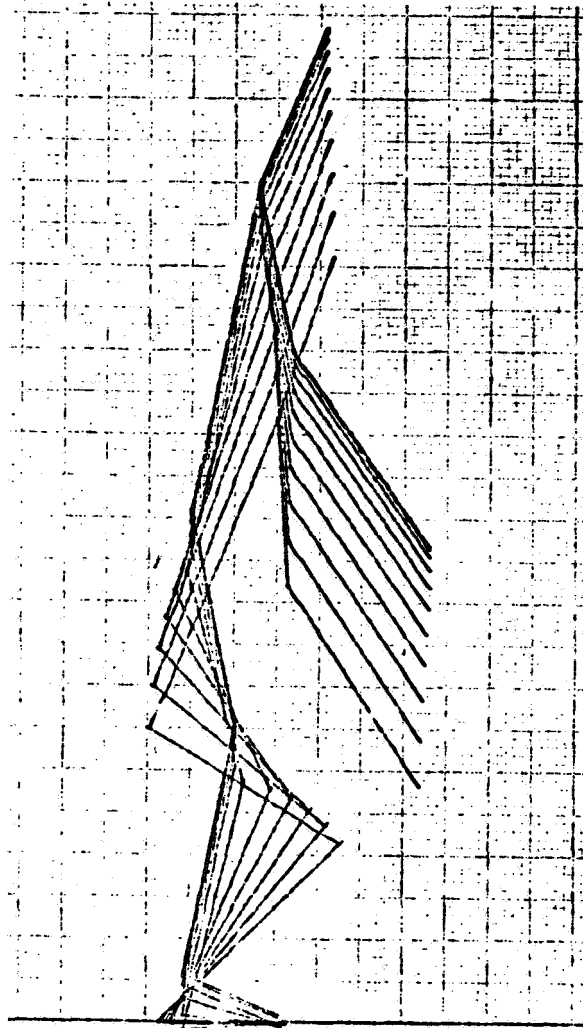


FIGURE 5.—Simulation results: free fall with no muscle torques.

Therefore the behavior indicated in figure 5 would continue until either the knee or the hip touched the ground—at which point the simulation would become invalid, since the possibility of ground reaction forces at these points has not been included in the model.

The principal value of figure 5 is verification of the ground reaction force simulation. Numerical data pertinent to figure 5 are given in table 3.

Strip chart recordings (figs. 6 and 7) of key variables depict the sequence of events with greater clarity. The initial free fall is clearly visible in the parabolic nature of y_T . When $y_T = 0$

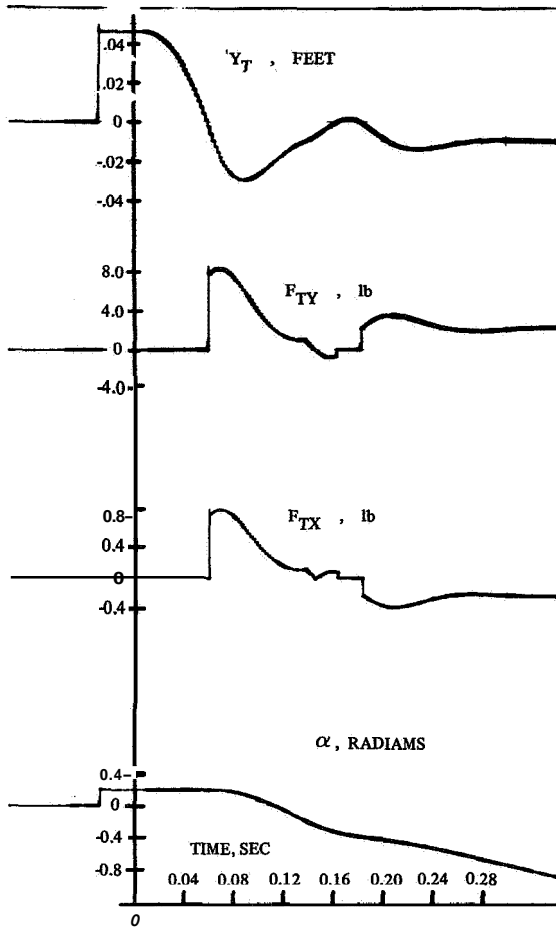


FIGURE 6.—Strip chart recordings of free-fall data: toe forces and angles.

(first contact with the ground), F_{TY} is seen to jump discontinuously to 8 lb and then decrease as sufficient angular velocity is imparted to the foot to cause the toe to rest gently slightly below the ground. Similar behavior is observed for the heel-ground interaction in figure 7.

Simulation Results : Free Fall with Subsequent Stand Erect

In this case, it is desired to use the muscle torques to cause the model to come to rest in an upright position after being dropped from an initial position slightly above ground. The model is initially in a flexed attitude with all muscle torques set equal to zero as long as $y_T > 0$ (the toe

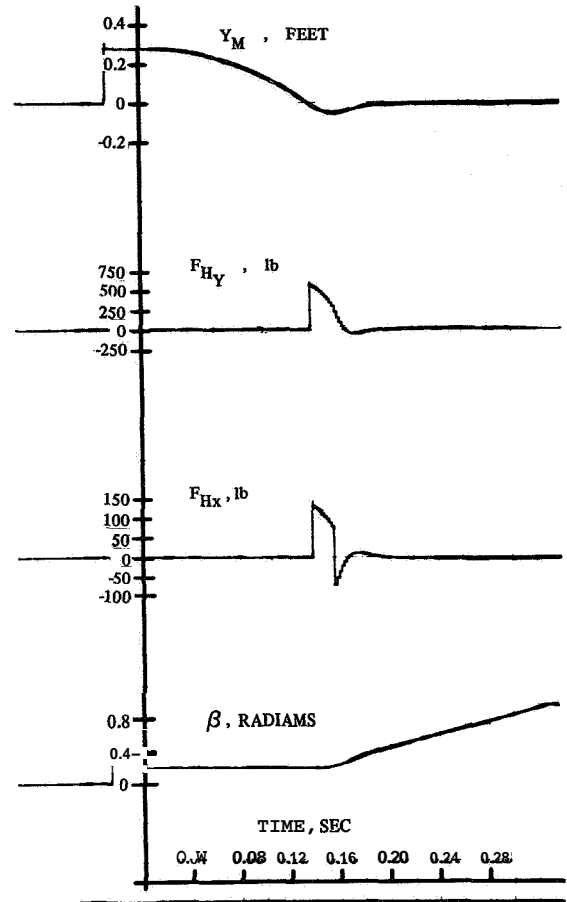


FIGURE 7.—Strip chart recordings of free-fall data: heel forces and knee angle.

is above ground). When the toe touches ground, the following form of *control law* is assumed, expressing muscle torques in terms of joint angles and angular rates,

$$T_\gamma = K_\gamma \gamma + K_{\dot{\gamma}} \dot{\gamma} \quad (11)$$

$$T_\beta = K_\beta \beta + K_{\dot{\beta}} \dot{\beta} \quad (12)$$

$$T_\alpha = K_\alpha \alpha + K_{\dot{\alpha}} \dot{\alpha} \quad (13)$$

$$T_\delta = K_\delta \delta + K_{\dot{\delta}} \dot{\delta} \quad (14)$$

$$T_\epsilon = K_\epsilon \epsilon + K_{\dot{\epsilon}} \dot{\epsilon} \quad (15)$$

$$T_\zeta = K_\zeta \zeta + K_{\dot{\zeta}} \dot{\zeta} \quad (16)$$

in the (possibly forlorn) hope that by attempting to drive all angles to zero the model will assume



FIGURE 8.—Simulation results: free fall with subsequent stand erect.

its reference position. Note, however, that the torques as given by equations (11) through (16) exhibit no dependence on the inertial trunk angle θ ; it is therefore quite possible for the model to line out in an inclined position relative to horizontal. The rate feedback terms are included to provide damping to stabilize the system.

Figure 8 presents pictorial results obtained using the control law of equations (11) through (16), with numerical values for the coefficients as specified in table 4. The time increment between drawings is 90 msec, and the results have been de-superimposed for clarity. The initial conditions are the same as for figure 7. The tendency to assume an erect position is clearly evident—which is somewhat surprising considering the complexity of the system and the ad hoc nature of the control law.

Simulation Results: The Graceful Leap

As a final result, figure 9 shows the model behavior when given an initial translational velocity in x , and with the control law of equation

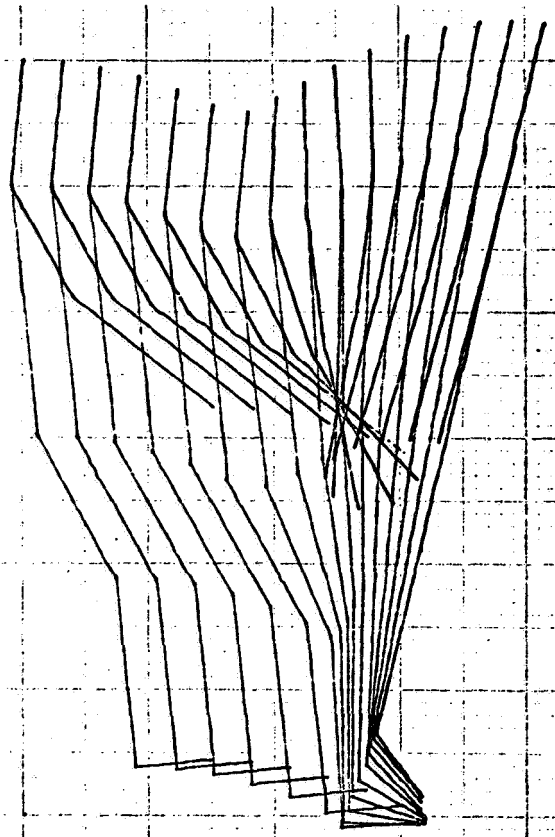


FIGURE 9.—Simulation results: the graceful leap.

TABLE 3.—Numerical Data for Figure 5: Free Fall

Initial conditions	Parameter values
$x(0) = 0.0$ ft	
$y(0) = 4.2$ ft	$k_T = -100.0$ (lb-ft)/rad
$\theta(0) = 0.2$ rad	$\dot{k}_T = -2.0$ (lb-ft)/(rad/sec)
$\gamma(0) = 0.4$ rad	$\mu_T = 0.21$
$\beta(0) = 0.4$ rad	$k_H = -5000.0$ (lb-ft)/rad
$\alpha(0) = 0.2$ rad	$\dot{k}_H = -125.0$ (lb-ft)/(rad/sec)
$\delta(0) = 0.4$ rad	$\mu_H = 0.23$
$\epsilon(0) = 0.4$ rad	
$\zeta(0) = 0.2$ rad	

(13) modified to

$$T_\alpha = K_\alpha(\alpha - 0.7) + K_\delta \dot{\alpha} \tag{17}$$

which has the effect of causing the foot to flex strongly toward an angle of 0.7 rad (about 40°) with respect to the perpendicular to the shank. The form of the other torque equations is left

TABLE 4.—Numerical Data for Figure 8: Xstand UP

Initial conditions	Parameter values	
$x(0) = 0 \text{ ft}$	$k_T = -5000$	$k_H = -5000$
$y(0) = 4.2 \text{ ft}$	$\dot{k}_T = -100$	$\dot{k}_H = -150$
$\theta(0) = 0.2 \text{ rad}$	$\mu_T = 0.5$	$\mu_H = 0.5$
$\gamma(0) = 0.4 \text{ rad}$	
$\beta(0) = 0.4 \text{ rad}$	$K_\gamma = -1000 \text{ (ft-lb)/rad}$	$K_{\dot{\gamma}} = -10 \text{ (ft-lb)/(rad/sec)}$
$\alpha(0) = 0.2 \text{ rad}$	$K_\beta = -200 \text{ (ft-lb)/rad}$	$K_{\dot{\beta}} = -15 \text{ (ft-lb)/(rad/sec)}$
$\delta(0) = 0.4 \text{ rad}$	$K_\alpha = -500 \text{ (ft-lb)/rad}$	$K_{\dot{\alpha}} = -5 \text{ (ft-lb)/(rad/sec)}$
$\epsilon(0) = 0.4 \text{ rad}$	$K_\delta = -150 \text{ (ft-lb)/rad}$	$K_{\dot{\delta}} = -7 \text{ (ft-lb)/(rad/sec)}$
$\zeta(0) = 0.2 \text{ rad}$	$K_\epsilon = -60 \text{ (ft-lb)/rad}$	$K_{\dot{\epsilon}} = -3 \text{ (ft-lb)/(rad/sec)}$
$(0) =$	$K_\zeta = -90 \text{ (ft-lb)/rad}$	$K_{\dot{\zeta}} = -3 \text{ (ft-lb)/(rad/sec)}$

TABLE 5.—Numerical Data for Figure 9: The Graceful Leap

Initial conditions	Parameter values	
$X(0) = 0 \text{ ft}$	$K_T = -5000$	$K_H = -500$
$\dot{x}(0) = 10 \text{ ft/sec}$	$K_{\dot{x}} = -100$	$K_{\dot{H}} = -150$
$y(0) = 4.2 \text{ ft}$	$\mu_T = 0.5$	$\mu_H = 0.5$
$\theta(0) = -0.1 \text{ rad}$	
$\gamma(0) = 0.4 \text{ rad}$	$K_\gamma = -200 \text{ (ft-lb)/rad}$	$K_{\dot{\gamma}} = -25 \text{ (ft-lb)/(rad/sec)}$
$\beta(0) = 0.4 \text{ rad}$	$K_\beta = -900 \text{ (ft-lb)/rad}$	$K_{\dot{\beta}} = -75 \text{ (ft-lb)/(rad/sec)}$
$\alpha(0) = 0 \text{ rad}$	$K_\alpha = -350 \text{ (ft-lb)/rad}$	$K_{\dot{\alpha}} = -4 \text{ (ft-lb)/(rad/sec)}$
$\delta(0) = 0.4 \text{ rad}$	$K_\delta = -150 \text{ (ft-lb)/rad}$	$K_{\dot{\delta}} = -7 \text{ (ft-lb)/(rad/sec)}$
$\epsilon(0) = 0.4 \text{ rad}$	$K_\epsilon = -60 \text{ (ft-lb)/rad}$	$K_{\dot{\epsilon}} = -3 \text{ (ft-lb)/(rad/sec)}$
$\zeta(0) = 0.2 \text{ rad}$	$K_\zeta = -90 \text{ (ft-lb)/rad}$	$K_{\dot{\zeta}} = -3 \text{ (ft-lb)/(rad/sec)}$

unchanged. Clearly the form of equation (17) has been chosen to mimic to some degree the action of the foot in propelling the body into the air.

Numerical data pertinent to figure 9 is as in table 5.

SUMMARY AND CONCLUSIONS

The conclusion reached from the results obtained so far is that a linear simulation is of such restricted validity as to be almost useless. While a linear *analysis* might occasionally be of use, a nonlinear *simulation* now seems essential if further progress is to be made.

Although it was recognized that a nonlinear representation of the ground reaction forces would be necessary, it was hoped that the basic system dynamics could be linearized with attendant simplicity and ease of analog computer mechanization. This does not appear to be the case. However, figures 5, 8, and 9 make it

clear that reasonable simulation results can be obtained for this complex system.

It now appears that although the coordinate system chosen in figure 1 is in terms of those angles most likely to be physiologically instrumented, it is not the one that leads to the simplest set of equations of motion. The frequent occurrence in the derivation of inertial angles such as $(\gamma - \theta)$, $(\beta - \gamma - \theta)$, etc., suggests that a great deal of simplification would occur if inertial angles were used as generalized coordinates. An early task for future work is the development of a full nonlinear simulation in terms of inertial angles.

The present nonlinear simulation is slow. Extensive comparison of simulation results with experimental data taken on human subjects would be time-consuming and expensive. Unfortunately, there is no obvious way of speeding up the present simulation. It is hoped that the nonlinear simulation in terms of inertial angles will

be less complex and therefore faster. Improvement in the speed of the simulation is clearly a continuing goal for future work.

The ideal torquemotor assumption of equations (11) through (16) is greatly at variance with physiological fact. Clearly, before extensive work is done on more realistic control laws, it would be desirable to have a more realistic representation of the geometry and dynamics of the human muscle structure. Developing this representation is a priority item for future work, and some initial effort has already been made in this direction. In addition, a few minor improvements in the ground reaction forces need to be made.

It is important to realize that the hypothetical

control law described by equations (11) through (16) is entirely for the purpose of debugging the parts of the simulation describing basic system dynamics, and no assertion is made or implied that this form of control law has any basis in fact. Indeed, information on the form of the control law is the desired long term output of the present research.

REFERENCE

1. HILL, J. C.: A Dynamic Model of the Human Postural Control System. Vol. I, Final Report on Biosystems Engineering Research. NASA/ERC contract NGR-23-054-003, Oakland Univ., School of Engineering TR 70-5, Nov. 1970.